WEDGE ABSORBER DESIGN FOR THE MUON IONISATION COOLING EXPERIMENT

C. T. Rogers*
P. Snopok, L. Coney
A. Jansson

Abstract

In the Muon Ionisation Cooling Experiment (MICE), muons are cooled by ionisation cooling. Muons are passed through material, reducing the total momentum of the beam. This results in a decrease in transverse emittance and a slight increase in longitudinal emittance, but overall reduction of 6d beam emittance.

In emittance exchange, a dispersive beam is passed through wedge-shaped absorbers. Muons with higher energy pass through more material, resulting in a reduction in longitudinal emittance as well as transverse emittance. Emittance exchange is a vital technology for a Muon Collider and may be of use for a Neutrino Factory. Emittance exchange has also been proposed as a technique to be used in the production of neutrons for Hadronic cancer therapy and in the manufacture of unstable rare isotopes for neutrino beam creation in the Betabeam scenario.

In this note, we study the cooling performance of different wedge materials and geometries and propose a set of measurements that would be made in MICE. We outline the resources these measurements would require and detail some of the engineering considerations and constraints that guide the choice of wedge parameters.

EMITTANCE EXCHANGE IN THE MUON IONISATION COOLING EXPERIMENT

Ionisation cooling is achieved in the Muon Ionisation Cooling Experiment (MICE) [1] baseline by the placement of absorbing material in the beamline. The absorbing material removes beam momentum, which is replaced only in the longitudinal direction by RF cavities, resulting in a net reduction of emittance. Low-Z materials must be used as absorbers together with carefully designed beam optics. This minimises the effects of multiple Coulomb scattering, which tend to reduce the cooling effect. Overall, transverse emittance is reduced to some equilibrium point while longitudinal emittance stays the same or increases slightly due to stochastic processes in the energy loss.

In this note we consider using MICE to observe a phenomenon known as emittance exchange. In emittance exchange a dispersive beam is passed through a wedge-shaped absorber. Muons with higher energy pass through more material and experience greater momentum loss. In this way the longitudinal emittance of the beam can be reduced either in addition to, or even instead of transverse emittance reduction. Emittance exchange is vital to a Muon Collider and has been considered as an upgrade option to the Neutrino Factory. Ring coolers [2], Helical coolers [3] and Guggenheim coolers [4] have been proposed to perform emittance exchange and longitudinal cooling using a simple wedge or a truncated wedge. Emittance exchange has been proposed as a technique for cooling beams in muon accelerators,

The proposed Guggenheim or RFoFo tilted solenoid ring system is closest to the system proposed in this note. In the Guggenheim lattice proposed for the muon collider, a beam with a dispersion of 80 mm is passed through liquid Hydrogen wedges with on-axis thickness of 280 mm and opening angle of 110°.

The measurement of longitudinal emittance reduction in MICE would:

- Demonstrate the accuracy of MICE's physics models for an absorber in a different geometry.
- Demonstrate that the physics of emittance exchange is well understood.
- Demonstrate emittance exchange in a real magnetic lattice.

It would be desirable to demonstrate emittance exchange and also energy replacement in a naturally dispersive lattice (i.e. with RF and dipoles), but that would be the subject of future work.

A first simulation study of wedges in MICE was made in [6], where it was shown that even a large emittance dispersive beam could be passed through MICE step IV without too serious non-linear effects given care in the way the beam is selected. Such a measurement had been discussed previously. In this note we go on to include some practical considerations and propose wedge geometries to be investigated in MICE. The measurements that would be made are discussed and the expected resources required are detailed.

Emittance Exchange

In this note the MICE Step IV geometry is considered in flip mode. The focussing system has symmetry in transverse planes x and y and the absorber is at an optical waist with no beam kinetic angular momentum. The dispersion function is assumed to also be at a waist and the dispersion direction aligned with the wedge. In this case the Courant-Snyder invariants can be shown to evolve in the presence of a wedge absorber according to [7] [8]

$$\frac{d\epsilon_x}{dz} = (1 - g_{//})\delta_p \epsilon_x + \chi_x \qquad (1)$$

* chris.rogers@stfc.ac.uk

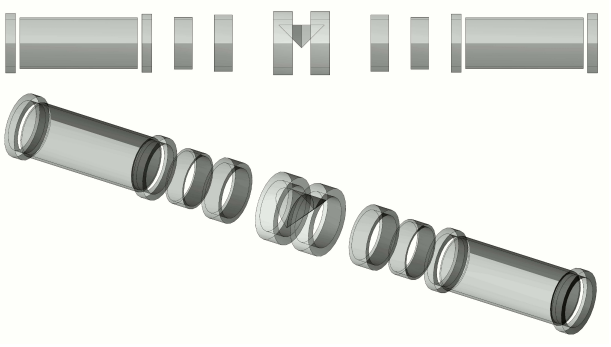

Figure 1: The geometry as simulated in G4MICE code: side and 3D view. The wedge absorber and coils are shown. The total length of the Step IV layout is just over 7.5 m, inner radius of the coils is 258 mm. A steel, cylindrical beam pipe with a 232 mm aperture was also included in simulations but is not shown in these figures.

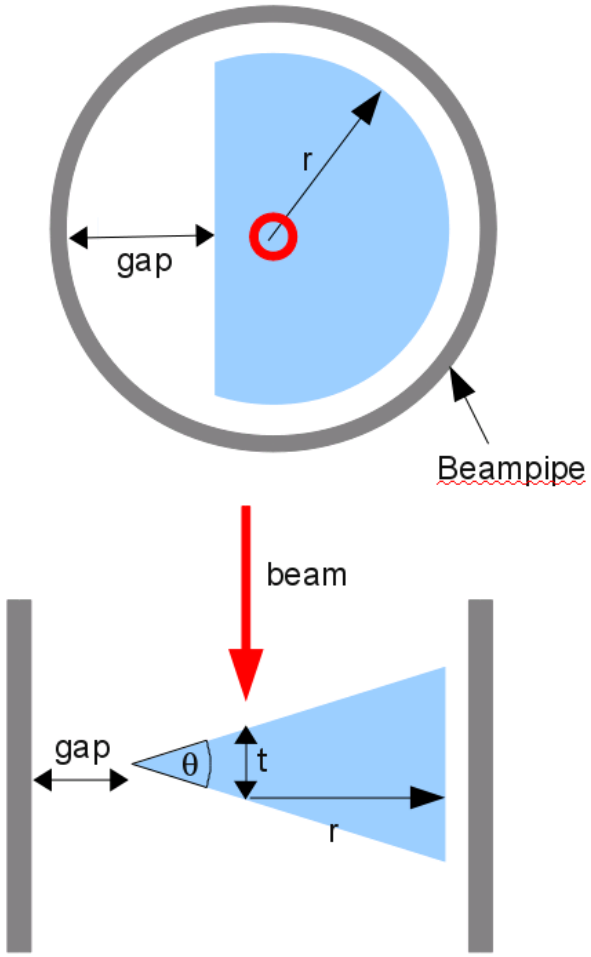

Figure 2: Schematic of the wedge geometry, which is parameterised by the on-axis thickness t, opening angle θ and radius r. In this picture the wedge is aligned on its side but this will not necessarily be the case in the final geometry.

$$\frac{d\epsilon_y}{dz} = \delta_p \epsilon_y + \chi_y \quad (2)$$

$$\frac{d\epsilon_{//}}{dz} = g_{//}\delta_p \epsilon_{//} + \chi_{//}, \quad (3)$$

where δ_p is the fractional change in momentum per unit length, $1/p\ dp/dz$ and χ_x, χ_y and χ_t are excitation terms given by

$$\chi_x = \frac{D_x^2}{2\beta_\perp}\frac{d\delta^2_{RMS}}{dz} + \frac{\beta_\perp}{2}\frac{d\theta^2_{RMS}}{dz} \quad (4)$$

$$\chi_y = \frac{\beta_\perp}{2}\frac{d\theta^2_{RMS}}{dz} \quad (5)$$

$$\chi_{//} = \frac{\beta_{//}}{2}\frac{d\delta^2_{RMS}}{dz} + \frac{D_x^2}{2\beta_{//}}\frac{d\theta^2_{RMS}}{dz}. \quad (6)$$

Here $\beta_\perp$ is the transverse Twiss function, $\beta_{//}$ is the longitudinal Twiss function, $d\theta^2_{RMS}/dz$ is the RMS multiple Coulomb scatter, $d\delta^2_{RMS}/dz$ is the RMS energy straggling and D_x is the dispersion, assumed to be aligned with the wedge. $g_{//}$ is a damping term given by

$$g_{//} = 1 - \frac{D_x}{\rho_0}\frac{d\rho}{dx} \quad (7)$$

where $\rho(x)$ is the thickness of the wedge and ρ_0 is the thickness of the wedge on-axis.

The six-dimensional emittance is given by the product of the two-dimensional emittances, $\epsilon_{6d} = (\epsilon_x\epsilon_y\epsilon_z)^{1/3}$. We note two points; the maximum damping rate, in the limit that stochastic effects are small and neglecting the curvature of the Bethe-Bloch relationship, is given by the Robinson criterion [9]

$$\frac{d\epsilon_{6d}}{dz} = \frac{2}{3}\delta_p\epsilon_{6d} \quad (8)$$

and the equilibrium six-dimensional emittance is given by setting the rate of change in each of the two dimensional emittances to 0.

$$\epsilon_{6d}^{eqm} = \left(\frac{\chi_x\chi_y\chi_{//}}{\delta_p^3 g_{//}(1-g_{//})}\right)^{1/3}. \quad (9)$$

Transverse Emittance

In a conventional accelerator with a naturally dispersive lattice, the decoupled emittances can be calculated using some eigenvalue analysis to diagonalise the transfer matrix. In MICE, the dispersion is introduced artificially (i.e. the beam is not periodic in the lattice) and so such an analysis is not appropriate. Instead, the emittances are defined as

$$\epsilon_{//} = \frac{\sqrt{det(\mathbf{V(ct,E)})}}{mc^2} \quad (10)$$

$$\epsilon_{6d} = \frac{\sqrt[6]{det(\mathbf{V(ct,E,x,p_x,y,p_y)})}}{m} \quad (11)$$

$$\epsilon_{4d} = \sqrt{\epsilon_{6d}^3/\epsilon_{//}} \quad (12)$$

where $\mathbf{V}$ is the covariance matrix of the specified space and $det(\mathbf{V})$ is the determinant of $\mathbf{V}$.

SIMULATION GEOMETRY

In this study a simple wedge-shaped absorber is simulated in a straight solenoid channel. The geometry considered is shown in Figure 1. The case considered here is MICE Step IV, where MICE is operated in a mode without RF cavities. The coil geometry is listed in Table 1; this is the baseline geometry as described in [10] but adapted for MICE Step IV. The only additional elements in the simulation are an aluminium beam pipe with a constant radius of 232 mm and the wedge descibed below.

The wedge is modelled by the intersection of a triangular prism with a cylinder, as shown in Figure 2. The wedge absorber is parameterised by the thickness on-axis that governs the energy lost by a reference particle, and the opening angle of the wedge, that governs the emittance exchange. For opening angles above about 30° and energy losses typical of MICE, the absorber does not fill the aperture, leaving a gap at the thin end of the wedge

Three materials are under consideration in this note, Lithium Hydride, Beryllium and Polyethylene. Lithium Hydride is a solid with low average Z and low Z/A resulting in less multiple scattering and energy straggling than Polyethylene for a given energy loss and hence a generally better cooling performance. Lithium Hydride is a restricted material as it can be used in the production of nuclear weapons, making it expensive and difficult to procure. There may also be some handling and safety issues associated with Lithium Hydride. Polyethylene is readily available and widely used for many industrial applications so is easy to procure and there are no handling issues specific to this material. Beryllium has significant handling and safety issues as Beryllium dust is toxic, but it is a material with comparable multiple scattering and energy straggling behaviour to the other materials considered in this note.

Wedge Requirements

In order to conclusively demonstrate longitudinal cooling, it is desirable that the longitudinal and six-dimensional emittance reduction is much greater than any optical beam heating due to the significant non-linearities involved in pushing a dispersive beam through a straight magnet system such as the one we have in MICE, and this is our primary criterion for the absorber. The second criterion is that the absorber has a good cooling performance, which tends to encourage the search for small equilibrium emittances for a range of beams. In addition, it is desirable to test candidate materials that may be used in a real six-dimensional lattice. In any study, the beam must have emittances that can be transported by MICE without excessive scraping and that can be generated by the beamline.

Available Beams

The MICE beamline has been designed with the aim of providing a number of different beam momenta and emittances in the range of 140 MeV/c to 240 MeV/c and 3 mm to 10 mm respectively. The MICE trackers can measure tracks with maximum radius of 150 mm. In the linear approximation this gives an acceptance of about 60 mm, which is an invariant with momentum. This corresponds to a maximum RMS emittance of order 10 mm. The MICE beamline is capable of filling this acceptance. The generation of lower emittance beams by the MICE beamline has not been demonstrated even in simulation, and this may put a practical constraint on the generation of beams below 6 mm.

Running with multiple beam line settings and combining datasets, it would then be possible to generate a dataset with momentum range 140 MeV/c to 240 MeV/c and emittances between 6 mm and 10 mm. This gives us a good range of parameters with which to populate phase space for beam selection. The slight caveat is that even if beam line settings were changed, it would be desirable to keep all MICE coils at constant current. So far beam matching has only been demonstrated at the 140 MeV/c momentum with 2.8 T in the tracker solenoid while 200 and 240 MeV/c matchings have been performed with 4 T in the solenoid. It is not foreseen that this will create serious difficulties.

Parameter	Value
Reference P [MeV/c]	200 [1]
Transverse emittance [mm]	6[2]
Transverse β [mm]	420
Transverse α	0
Longitudinal emittance [mm]	90
Longitudinal β [ns]	10
Longitudinal α	0
RMS Energy Spread [MeV]	25.1
D_x [mm]	200
D_y [mm]	0
D'_x	0
D'_y	0
Number of μ^+	10000

Table 2: Parameters of the simulated beam at the wedge centre. D_i, D'_i are the dispersions and their derivatives.

Control of dispersion has not been planned for the MICE beam line, and is expected to be challenging. It may be possible to introduce dispersion using a wedge-shaped disc in the diffuser mechanism, but achieving a satisfactory D and D' is probably not possible. For the purpose of this note, it is assumed that dispersion will be introduced using a beam selection algorithm.

The parameters of the beam that was used in simulation, corresponding to a beam matched to the canonical MICE lattice and with typical emittances, are listed in Table 2. A dispersion of 0.2 m was used in the simulation, which is approximately a factor 2 larger than the nominal dispersion

[1] At the lattice start.

[2] The transverse distribution was generated ignoring the effects of dispersion, such that the calculated emittance is different from the nominal emittance listed here.

Coil	Length [m]	Inner Radius [m]	Radial Thickness [m]	Mean Z [m]	Mean R [m]	Current [A/mm^2]
FC1	0.2100	0.2630	0.0840	0.205	0.3050	113.95
M1	0.2012	0.2580	0.0447	0.861	0.2804	118.56
M2	0.1995	0.2580	0.0298	1.30105	0.2729	137.13
E1	0.1106	0.2580	0.0596	1.701	0.2878	127.37
C	1.3143	0.2580	0.0213	2.45105	0.2687	152.44
E2	0.1106	0.2580	0.0660	3.201	0.2910	135.18

Table 1: Geometry of the simulated magnet elements. The geometry is reflected about $z = 0$ and polarities are reversed for coils with $z > 0$.

in the proposed muon collider Guggenheim channels that this lattice most closely resembles. The larger dispersion is needed for longitudinal emittance reduction in this case. A larger longitudinal emittance could be used, but the full MICE lattice has resonances at 150 MeV/c and 250 MeV/c that would restrict the cooling performance for larger longitudinal emittances.

Cooling Signal of Canonical Beam

The main criterion for wedge absorber choice is that a strong cooling signal be observable. The cooling signals for various wedges with the beam described above are shown in Figure 3. Polyethylene (C_2H_4), Beryllium (Be) and Lithium Hydride (LiH) materials were simulated with 60.5 mm, 40.2 mm and 75.4 mm respectively, corresponding to about 12 MeV energy loss at 200 MeV, and various opening angles. 12 MeV energy loss was chosen as it corresponds roughly to the energy loss in the standard MICE absorbers and is typical of ionisation cooling channel designs. In principle thicker absorbers could be used; the advantage is that any cooling signal may be more pronounced; the disadvantage is that this would take the absorber away from the parameter range normally considered for ionisation cooling channels and a significant energy loss may increase non-linear effects.

Longitudinal emittance reduction is more pronounced for larger wedge angles while transverse emittance reduction is more pronounced for lower wedge angles. For higher wedge angles, $\partial/\partial x(dE/dz)$ is more pronounced so that the longitudinal partition function is larger, resulting in more longitudinal cooling. For the same reason, more longitudinal cooling is observed for polyethylene than Lithium Hydride and more again in Beryllium; the relative Z/A in each material may lead to more energy straggling in Be and polyethylene, but this is outweighed by the increased energy loss that leads to greater $\partial/\partial x(dE/dz)$ for a given wedge angle. In most cases the wedges heat in transverse phase space, with more heating for larger opening angles. $\partial/\partial x(dE/dz)$ is larger and in the transverse case this leads to less cooling, while the radiation length in polyethylene and Beryllium is larger than Lithium Hydride leading to significant heating.

The key part of this experiment is to demonstrate longitudinal emittance reduction. In light of this, the 30° wedge is disfavoured for Lithium Hydride and polyethylene as the longitudinal cooling signal is too weak. On the other hand, the 30° Lithium Hydride wedge is interesting as there is both a transverse and longitudinal cooling signal. It may be possible to increase the dispersion to increase the longitudinal emittance reduction but this would take the lattice away from parameters that are currently foreseen in emittance exchange systems.

A concern for this experiment is the significant optical heating and cooling. The distinction of emittance change effects caused by the wedge from emittance changed effects caused by optical effects may be possible by projecting the beam measurement to immediately next to the wedge. The effect of such a projection on measurement error has not been studied.

Equilibrium Emittance

In choosing the opening angle of the wedge and wedge material, one consideration is the equilibrium emittance of the wedge and lattice. Beams below equilibrium emittance are heated and beams above this emittance are cooled. In a more conventional 6d cooling lattice, the equilibrium emittance is uniquely defined by the field map, the wedge material and opening angle, and the requirement that the beam be matched (periodic with the lattice cell). In the lattice described here the match condition would result in a dispersion of zero; by using a non-zero dispersion the match condition is deliberately broken for this parameter only, making dispersion a free parameter.

In Figure 4 the equilibrium emittance for various wedge parameters is calculated as a function of dispersion. Two algorithms were used to calculate the equilibrium emittance. A semi-analytical model was used where the action of the physics processes appropriate for a wedge was calculated on a beam with an appropriate dispersion. A two-dimensional numerical root-finding routine was applied to find the point where longitudinal and 6d emittance was conserved, as a function of the input longitudinal and 6d emittance. This was plotted as a line in Figure 4. This calculated point was then used as a seed to find the equilibrium emittance; beams above, below and at the equilibrium emittance were tracked through a wedge and a two-dimensional linear regression was applied to find the equilibrium emittance. Each of these Monte Carlo batch jobs is shown as a

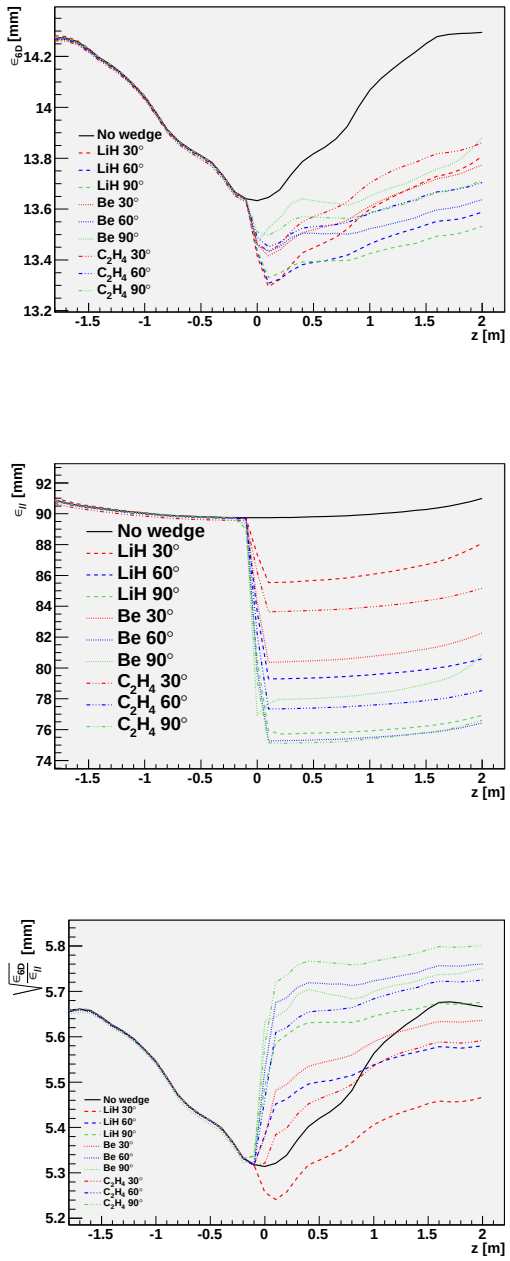

Figure 3: Simulated emittance along the beamline for canonical beam parameters and a dispersion of 200 mm.

point in Figure 4.

In general, the simulated data reflects the analytical model reasonably well. The analytical model estimates a consistently larger equilibrium emittance for higher dispersions. Some of the points at the largest and smallest dispersions are somewhat suspect; in some of these cases the root-finding algorithm failed to converge, presumably because the equilibrium longitudinal emittance was very large. In particular for the high-dispersion cases, it is not clear that it will be possible to achieve such a strong correlation in MICE. Weighting algorithms have only been studied for cases below 200 mm.

The equilibrium emittance is in general smaller for smaller $\partial/\partial x(dE/dz)$. Lithium Hydride has the smallest equilibrium emittances, in part owing to the smaller multiple scattering and energy straggling. Additionally the large dE/dx of the higher Z materials leads to increased $\partial/\partial x(dE/dz)$.

Minimum Wedge Radius

In this section the effect of a constraint on wedge radius is examined. The inner radius of the focussing coil in the MICE AFC module is 263 mm, the bore of the beam pipe has an inner radius of 235 mm and mounting flanges for the absorbers intrude to an inner radius of 160 mm. A schematic of the absorber focus coil is shown in Figure 5.

The effect of limiting the wedge absorber radius on emittance change is shown in Figure 6 for a 6 mm beam with 200 mm dispersion. As in all simulations, the bore of MICE was assumed to be 232 mm. The radius of the absorber was lowered from 225 mm, considered to be the largest that could fit inside the bore, and the fractional change in emittance was studied. For these simulations, a Lithium Hydride wedge with 90° opening angle was simulated. Below 150 mm, the cooling performance of the wedge is degraded. Referring to the schematic of the AFC, the lowest radius aperture is the mounting flange that comes in to 160 mm radius. This indicates that the aperture of the AFC is sufficient for a 6 mm beam, but that the wedge radius should be kept above about 150 mm.

Effect of Wedge-Aperture Gap

The distribution in x-position for a gaussian beam of 6 mm transverse emittance is shown in Figure 7 superimposed over the wedge half-thickness for the wedges considered above. It is clear that part of the beam does not pass through the wedge at all for some wedges. This is worse for thinner wedges, wedges with higher opening angles and beams with larger transverse emittance.

In Figure 8 the cooling performance of the beam is assessed in terms of particle ampltidue. Particle amplitude is a measure of how far particles are from the beam centre, defined by

$$A_n = \epsilon_n \vec{u}_n^T \mathbf{V_n^{-1}} \vec{u_n} \tag{13}$$

where ϵ_n is an invariant emittance, $\vec{u}_n$ is the phase space

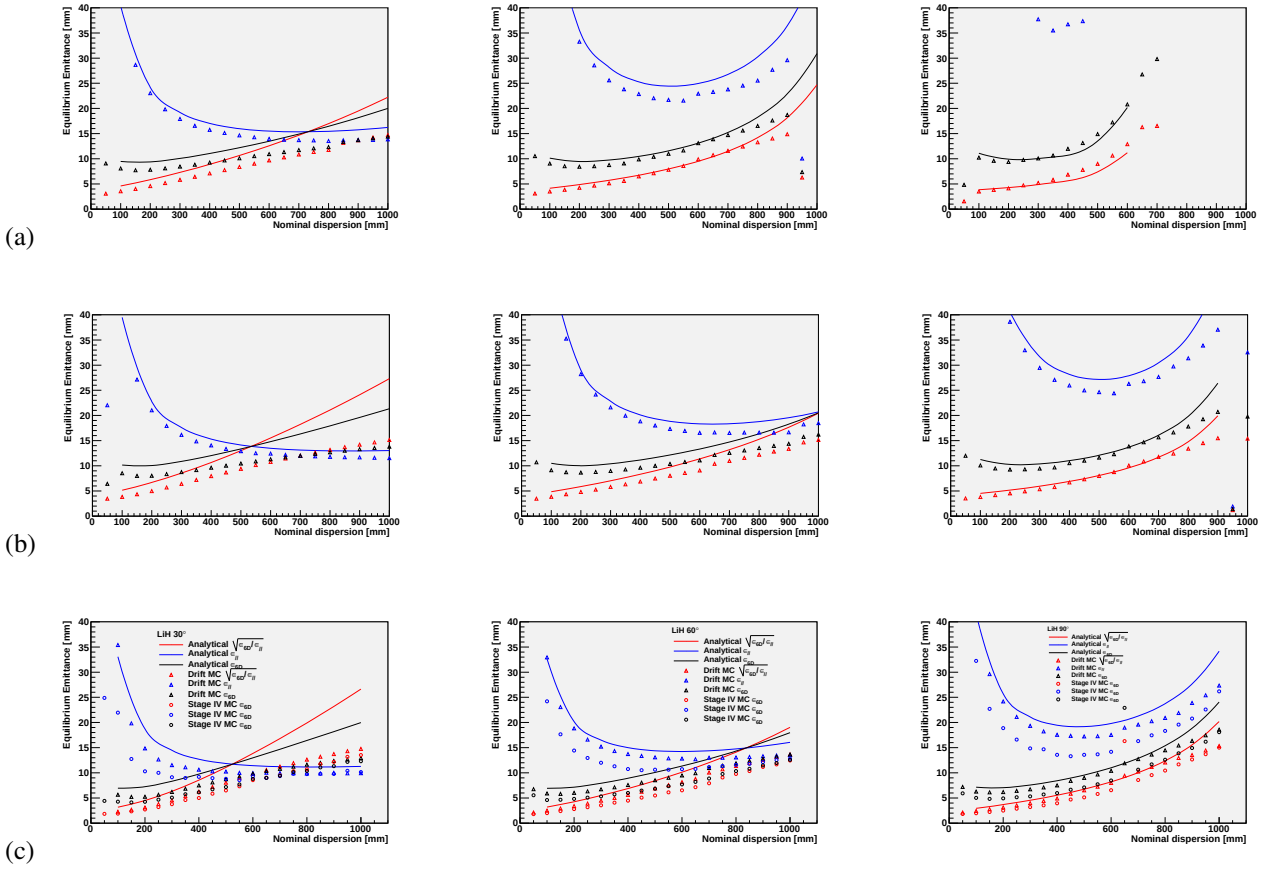

Figure 4: Equilibrium emittance for various wedge geometries and materials. Lines are calculated equilibria, while triangular points are generated from Monte Carlo simulation of a wedge in the absence of fields. For the Lithium Hydride wedge, circular points show Monte Carlo simulation through the full Stage IV field map. The 6d, 4d and 2d emittances are plotted in black, red and blue respectively. In row (a) Beryllium was modelled, in (b) polyethylene and in row (c) Lithium Hydride was used. The opening angle θ is 30°, 60° and 90° for left-most, middle and right-most columns respectively.

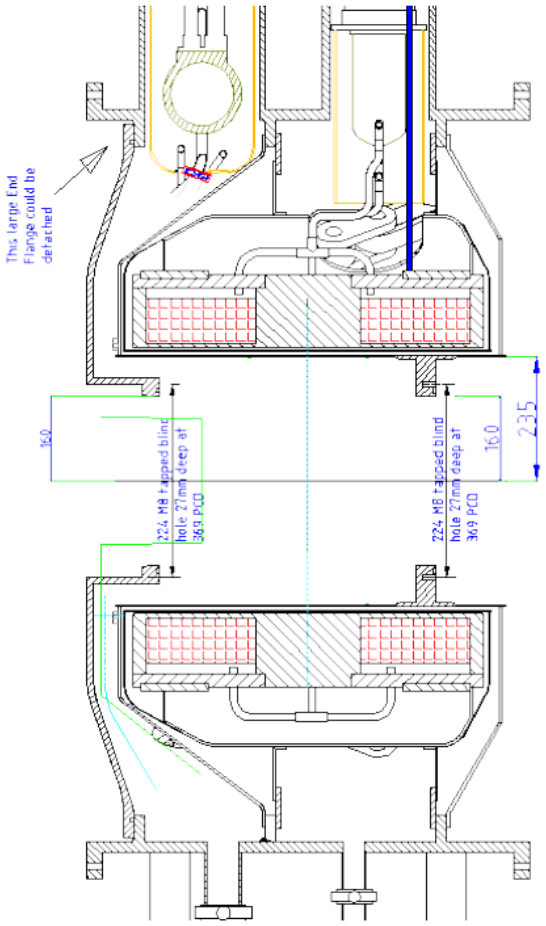

Figure 5: Schematic of the Absorber Focus Coil geometry (courtesy W Lau).

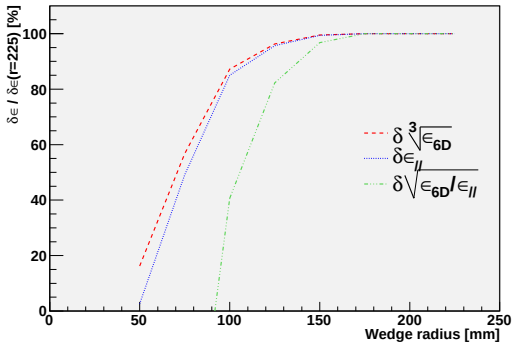

Figure 6: Effect of reducing the outer radius of the wedge on the emittance change.

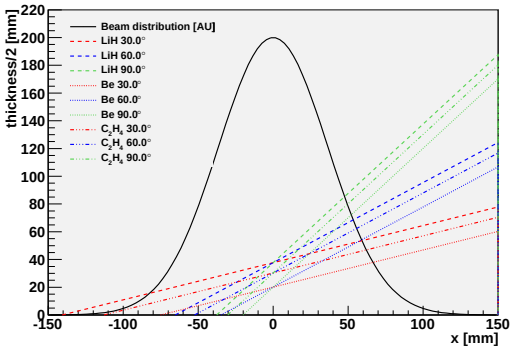

Figure 7: Wedge absorber geometry and beam distribution at 6 mm transverse emittance.

of the invariant and $\mathbf{V_n}$ is the covariance matrix associated with that invariant. By analogy with the emittances discussed above, it is not appropriate to define a transverse amplitude in this case. Instead we assume that it is possible to define a rotation that decouples transverse and longitudinal phase spaces, such that we can write $\vec{u}_{6d} = (\vec{u}_{2d}, \vec{u}_{4d})$ and

$$\mathbf{V_{6d}} = \begin{pmatrix} \mathbf{V_{2d}} & 0 \\ 0 & \mathbf{V_{4d}} \end{pmatrix}. \tag{14}$$

Then the 4d transverse amplitude can be written in terms of the 6d and 2d longitudinal amplitude as

$$A_{4d} = \epsilon_{trans} \left(\frac{A_{6d}}{\epsilon_{6d}} - \frac{A_{2d}}{\epsilon_{//}} \right) \tag{15}$$

where ϵ_{trans} is also calculated using 2d and 6d emittances as outlined in (10).

In Figure 8, the number of muons at input and output is plotted against particle amplitude for a 6 mm beam with 200 mm dispersion traversing a Beryllium absorber with 90° opening angle and 40.2 mm thickness on axis. In addition, the ratio of these histograms is plotted. Where the ratio is greater than 1, the number of muons at a particular amplitude has increased. The RMS emittance is related to the mean amplitude by [12]

$$\epsilon_i = \frac{< A_i >}{2N} \tag{16}$$

where N is the number of dimensions of the phase space. So increase in the number of particles in an amplitude bin above the $< A_i > /2N$ indicates a growth in RMS emittance, while increase in the number of particles in an amplitude bin below $< A_i > /2N$ contributes to the reduction in RMS emittance.

Two sets of plots are included; in the first instance the distribution is plotted including all particles, while in the second instance the distribution is plotted but adding only muons that pass through the wedge. In both cases the covariance matrix for the full beam is used to calculate amplitudes. About 71% of the beam passes through the wedge.

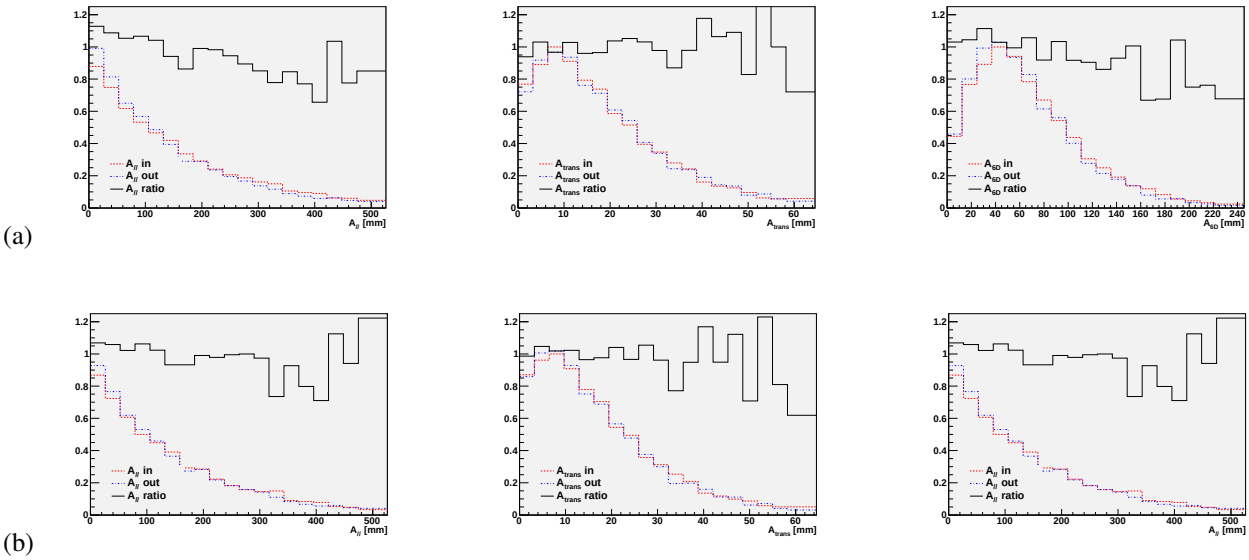

Figure 8: Distribution of particle amplitudes after traversing a 90° Beryllium absorber and Step IV fields (normalised). In row (a) all particles are added to the histogram, while in row (b) only particles that traverse the absorber are added. The 'ratio' plot is the ratio of number of particles in a bin at output to number of particles in a bin at input.

More longitudinal cooling is evident and less transverse heating in the case where all muons are included. Overall the 6d cooling performance is better when only muons that traverse the wedge are counted, but the effect of the wedge-aperture gap is not too detrimental.

Wedge Choice

As discussed above, the choice of wedge to operate is determined by the longitudinal emittance change that will be observed and the equilibrium emittance that can be achieved. The 90° Lithium Hydride wedge is favoured as it shows the largest longitudinal emittance reduction. As demonstrated, the wedge-absorber gap is not thought to affect the emittance change; however, it may make some analyses more complicated. The 30° Lithium Hydride wedge is of interest as it has a good longitudinal equilibrium emittance enabling a broader range of parameters to be studied, and also covers most of the AFC aperture. The 60° Lithium Hydride wedge would then complete the set. It would also be interesting to study 30°, 60° and 90° of polyethylene wedges as a cross-check of the physics process model, dependent on the time available for this experiment.

Rejected Options

The following options for absorbers have been considered and rejected, principally because of cost or difficulty.

- Automated absorbers, which would enable the changing of parameters such as angle of rotation along the beam axis or opening angle, have been rejected. Such a system would be required to operate in vacuum and strong magnetic fields. Designing, constructing and testing such a device would be challenging.
- Exotic shaped absorbers, which would enable the matching of energy loss in the absorber to the natural energy-position correlations in the beam, have been rejected. This system would require knowledge of the beam in advance of manufacture, which is not practical. In addition, simulation studies have indicated that there will be correlations between energy and transverse momentum that could not be removed by such an absorber, so some beam selection algorithm would be necessary in any case.
- Liquid Hydrogen absorbers are not foreseen as being practicable on the timescale of this experiment. Several years of R&D have been performed in order to realise the canonical MICE Hydrogen absorbers, and much of the work would have to be redone for wedge shaped absorbers.

PRACTICAL CONSIDERATIONS

Absorber Engineering

At the time of writing, a request is in preparation for an estimate from Y12 for the 3 LiH absorbers described above. Some engineering support would be required for the construction of polyethylene absorbers.

The mass and dimensions of each absorber simulated in this note are listed in Table 3. We would like to be able to mount the absorber so that the wedge is aligned with natural dispersion in the beam. Owing to uncertainty in the actual beam that MICE will get, this means that we would

material	LiH	LiH	LiH	C_2H_4	C_2H_4	C_2H_4	Be	Be	Be
θ [°]	30	60	90	30	60	90	30	60	90
r [mm]	225.0	225.0	225.0	225.0	225.0	225.0	225.0	225.0	225.0
t [mm]	75.4	75.4	75.4	60.5	60.5	60.5	40.2	40.2	40.2
h [mm]	365.7	290.3	262.7	337.9	277.4	255.3	300.0	259.8	245.1
l [mm]	98.0	167.6	225.0	90.5	160.2	225.0	80.4	150.0	225.0
d [mm]	0	0	37.7	0	0	25.1	0	0	20.1
mass [kg]	12.16	16.27	17.7	12.4	17.3	19.0	20.5	30.6	34.2

Table 3: Parameters of the wedges described in this note. Dimensions are labelled in Figure 9.

like to be able to mount the wedge at any angle in the AFC, possibly leading to significant torque that will need to be supported. Any mounting structure would need to leave the central 160 mm radius aperture of the AFC free of material. The absorber mounting has 24-fold symmetry enabling the wedge to be mounted at any angle that is an integer multiple of $15°$.

As shown in Figure 5, two mounting flanges for the absorber intrude into the AFC module to an inner radius of 160 mm. These would interfere with the $90°$ wedges, so it will be necessary to restrict the maximum length of the wedges to 450 mm. This should not affect the wedge inside the 160 mm inner radius. A transverse section of the modified wedge is shown in Figure 9.

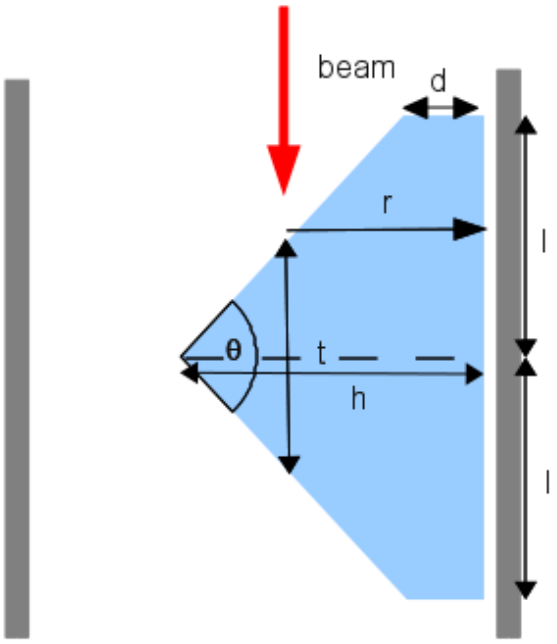

Figure 9: Schematic of the modified wedge with a cut-off where the wedge interferes with the AFC flanges.

Experimental Procedure

For each absorber, we would like to run over a range of beam emittances to fully populate phase space for any weighting algorithm. It may be of interest to investigate the use of non-flip mode to reduce non-linear optical effects or operate at alternate momenta, although at present this is not foreseen in our experimental programme. For each wedge, we would have to

- Install the wedge. This would take 4-14 days.
- Run at each of 3 beam emittances. Each run of 1e6 events would take 6 hours or one shift, assuming a somewhat pessimistic event rate of 50 Hz. Assuming one shift per day this would take 3 days.

Each absorber would require two to three weeks for installation and measurement. Beam selection is planned explicitly to be performed during analysis.

Owing to the experiment's reliance on weighting algorithms, a formal blinding procedure is envisaged.

- A run of events would be measured. From this run a small subsample of events would be taken and stored in an unblinded manner, while the main body of events would have upstream and downstream detector data stored separately and initially the downstream detector data would not be accessible to experimenters.
- The unblinded data would be analysed and checked for data integrity.
- The upstream detector data would be reconstructed to recover phase space position and upstream PID of each event at the upstream Tracker Reference Plane. Incoming beam contaminations would be rejected.
- Statistical weights would be applied.
- The downstream detector data would be reconstructed to recover phase space position of each event at the Tracker Reference Plane and downstream PID. Downstream beam contaminations (decay electrons) would be rejected.
- Emittance change, amplitude analysis and any other analyses would be performed.

This places some requirements on the software and hardware.

CONCLUSION

A detailed study has been made to enable choice of a wedge for placement in MICE. The cooling performance for a canonical beam and equilibrium emittance over a range of beam dispersions has been studied. This has led to the choice of, ideally, 30°, 60° and 90° Lithium Hydride wedges and an equivalent set of plastic wedges.

REFERENCES

[1] D. Li, Status of the International Muon Ionization Cooling Experiment (MICE), Proc. COOL 2009.

[2] V. Balbekov, Solenoid-Based Ring Coolers, MUCOOL Note 232, 2002.

[3] K. Yonehara, Progress of Helical Cooling Channel Design for Muon Colliders, Proc. COOL 2009.

[4] P. Snopok, G. Hanson, A. Klier, Recent Progress on the 6d Cooling Simulations in the Guggenheim Channel, International Journal of Modern Physics A, Volume 24, Issue 05, 2009.

[5] K. Okabe, Y. Mori, An Intense Neutron Source with Emittance Recovery Internal Target (ERIT) Using Ionization Cooling, Proc. EPAC 2008.

[6] C. T. Rogers, P. Snopok, Wedge Absorber Simulations for the Muon Ionization Cooling Experiment, Proc. COOL 2009.

[7] D. Neuffer, Introduction to Muon Cooling, NIM A 532, 2004.

[8] C. Wang, K. Kim, Beam-envelope Theory of Ionization Cooling, NIM A 532, 2004.

[9] K. W. Robinson, Radiation Effects in Circular Electron Accelerators, Phys. Rev. 111, 1958

[10] U. Bravar, J. H. Cobb, J. Rochford, C. T. Rogers, The Effect of Error Fields due to Hall Shielding on the Performance of MICE, MICE Note 244.

[11] C. T. Rogers, Statistical Weighting of the MICE Beam, Proc. EPAC 2008.

[12] C. T. Rogers, Beam Dynamics in an Ionisation Cooling Channel, Thesis, 2007.